Interaction Enhanced Imaging of Individual Rydberg Atoms in Dense Gases

G. Günter, M. Robert-de-Saint-Vincent, H. Schempp, C. S. Hofmann, S. Whitlock,* and M. Weidemüller†

Physikalisches Institut, Universität Heidelberg, Philosophenweg 12, 69120 Heidelberg, Germany

(Received 27 June 2011; revised manuscript received 8 November 2011; published 5 January 2012)

We propose a new all-optical method to image individual Rydberg atoms embedded within dense gases of ground state atoms. The scheme exploits interaction-induced shifts on highly polarizable excited states of probe atoms, which can be spatially resolved via an electromagnetically induced transparency resonance. Using a realistic model, we show that it is possible to image individual Rydberg atoms with enhanced sensitivity and high resolution despite photon-shot noise and atomic density fluctuations. This new imaging scheme could be extended to other impurities such as ions, and is ideally suited to equilibrium and dynamical studies of complex many-body phenomena involving strongly interacting particles. As an example we study blockade effects and correlations in the distribution of Rydberg atoms optically excited from a dense gas.

DOI: 10.1103/PhysRevLett.108.013002 PACS numbers: 32.80.Rm, 32.30.Jc, 42.50.Gy

The ability to prepare and probe individual quantum systems in precisely controlled environments is a driving force in modern atomic, molecular, and optical physics. Manipulating single atoms [1], molecules [2], and ions [3], for example, is becoming a common practice. At the heart of these experiments are powerful imaging techniques, which have taken on great importance in diverse areas, such as chemical sensing and chemical reaction dynamics [4], probing superconducting materials [5], and for quantum logic and quantum information processing [6]. Recently, new single atom and single site sensitive imaging techniques for optical lattices have opened the door to control and probe complex many-body quantum systems in strongly correlated regimes [7].

The usual approach to detect single particles is to measure the fluorescence or absorption of light by driving a strong optical cycling transition. Weak or open transitions present a difficulty since the maximum number of scattered photons becomes greatly limited. In the case of long-lived states of trapped ions, electron shelving has been used as an amplifying mechanism in order to directly observe quantum jumps [8]. Another approach involves the use of an optical cavity to enhance the interaction of atoms with a light field [9]. This makes it possible to reach single-atom sensitivity, but usually at the expense of greatly reduced spatial resolution.

Here we propose a new approach to imaging individual particles, by exploiting their interaction with a bath of easily interrogated probe atoms. Interactions alter the properties of a strong optical transition for many probe atoms within a critical radius, thereby providing two mechanisms which greatly enhance the effect of a single impurity on the light field. This approach could be used to study the effects of impurities and disorder on superfluids [5], to realize high-fidelity readout of atomic quantum registers [6], or as a precise way to observe individual charges or defects near surfaces [10]. As a probe we consider interaction-induced shifts of highly polarizable Rydberg states of a dense atomic gas, resolved via a narrow electromagnetically induced transparency (EIT) resonance. Even though the Rydberg states are barely populated, the EIT resonance is extremely sensitive to their properties [11,12], thereby providing the means to obtain a strong absorption signal and great sensitivity combined with high spatial resolution for detecting individual impurities.

We exemplify our scheme for the specific case of imaging many-body states of strongly interacting Rydberg atoms which act as impurities in a quasi-two-dimensional atomic gas (depicted in Fig. 1). Rydberg atoms are of great interest because their typical interaction ranges are

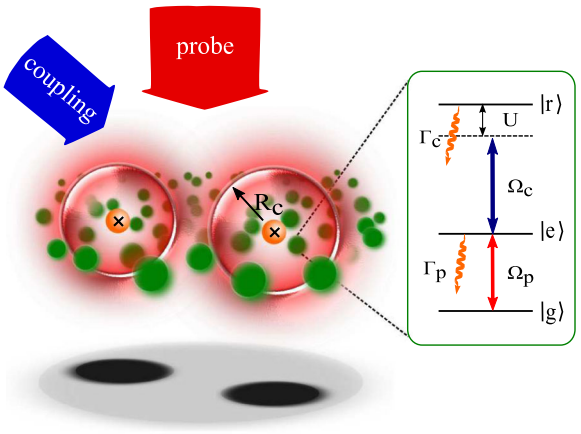

FIG. 1 (color online). Scheme for imaging individual impurities within a dense atomic gas. Impurity particles (crosses) are embedded within a dense two-dimensional atomic gas of probe atoms. The probe atoms interact with two light fields (coupling and probe) via a two-photon resonance with an excited state $|r\rangle$. This produces an EIT resonance on the lower transition. However, strong interactions with an impurity lead to a frequency shift U of the resonance within a critical radius R_c. The change in absorption properties of many surrounding atoms makes it possible to map the distribution of impurities to the absorption profile of a probe laser for analysis.

comparable to, or larger than, the typical interatomic separations in trapped quantum gases. Traditionally Rydberg atoms are field ionized and the resulting ions are subsequently detected. This is inherently destructive, has relatively poor overall detection efficiency, and typically has limited spatial resolution. As a result, much of the work done so far, such as the scaling laws for excitation [13], excitation statistics [14], and light-matter interactions [11], has been restricted to the study of cloud averaged properties. Only recently [15] have spatial correlations of Rydberg gases been imaged using field ion microscopy. A better approach would be to optically detect the Rydberg atoms; however, they have no suitable probe transition. Müller *et al.* proposed that a single Rydberg atom could control the optical transfer of an ensemble of ground state atoms between two states using the Rydberg blockade [16], which could also be used for detection [17].

We present a simple method that exploits the strong interactions with a bath of atoms to realize nondestructive single-shot optical images of Rydberg atoms with high resolution and enhanced sensitivity. We anticipate this technique will complement the new optical lattice imaging techniques [7], but with the capability to directly image many-body systems of Rydberg atoms. We show, in particular, that this will provide immediate experimental access to spatial correlations in recently predicted crystalline states of highly excited Rydberg atoms [18]. In contrast to field ionization, this approach does not destroy the many-body Rydberg state and in principle allows for the study of the time evolution of a single sample.

To describe the absorption of light by a gas of probe atoms surrounding a Rydberg atom we follow an approach based on the optical Bloch equations [19]. The Hamiltonian describing the atom-light coupling is

$$H_0 = \frac{\hbar}{2}(\Omega_p|e\rangle\langle g| + \Omega_c|r\rangle\langle e| + \Delta_p|e\rangle\langle e| + (\Delta_p + \Delta_c)|r\rangle\langle r| + \text{H.c.}). \quad (1)$$

For resonant driving ($\Delta_p = \Delta_c = 0$) a dark state $|\text{dark}\rangle \approx \Omega_c|g\rangle - \Omega_p|r\rangle$ is formed, which no longer couples to the light field. Consequently, the complex susceptibility χ of the probe transition vanishes and the atoms become transparent.

The presence of a nearby Rydberg atom in a different state causes an energy shift $U = \hbar C_6/|d|^6$ for the state $|r\rangle$, where d is the distance to the Rydberg atom and the interaction coefficient C_6 reflects the sign and strength of interactions on probe atoms in the $|r\rangle$ state. One should also account for interactions between atoms in state $|r\rangle$, but these can be neglected for $\Omega_p \ll \Omega_c$ when the population in $|r\rangle$ becomes small. We also include spontaneous decay from the states $|e\rangle$ and $|r\rangle$ with rates Γ_p, and Γ_c, respectively. From the master equation for the density matrix ρ we solve for the complex susceptibility of the lower probe transition.

In the weak probe limit ($\Omega_p \ll \Omega_c, \Gamma_p$) we assume the population stays mostly in the ground state ($\rho_{gg} \approx 1$). In this case we obtain for the susceptibility

$$\chi = \frac{i\Gamma_p}{(\Gamma_p - 2i\Delta_p) + \Omega_c^2(\Gamma_c - 2i\Delta)^{-1}}, \quad (2)$$

where $\Delta = \Delta_p + \Delta_c + C_6/|d|^6$.

Figure 2 shows the imaginary part of χ, which is proportional to the probe absorption, for different laser parameters and for different distances d to a Rydberg atom. Far from the influence of the Rydberg atom ($d \to \infty$), the susceptibility takes on a characteristic shape with vanishing absorption on resonance. For smaller distances, the EIT resonance shifts due to Rydberg-Rydberg interactions, and the on-resonant absorption starts to increase. For $d \to 0$, the excited states $|r\rangle$ become far detuned and the background atoms effectively act as two-level systems. In this case the usual Lorentzian line shape is recovered with maximum absorption on resonance. Hence, for a two-dimensional atomic gas with density n_{2D}, the presence of a Rydberg atom triggers $N = n_{2D}\pi R_c^2 \gg 1$ atoms (each with an absorption cross section $\sim\lambda^2$) to scatter many photons, thereby producing a dark shadow on the probe beam. From Eq. (2) and taking $\Delta_p = \Delta_c = 0$ and $\Gamma_c \approx 0$ we find the distance dependent susceptibility $\text{Im}[\chi] \approx [1 + (d/R_c)^{12}]^{-1}$ where we have defined a critical distance $R_c = (2C_6\Gamma_p/\Omega_c^2)^{1/6}$, at which $\text{Im}[\chi]$ reduces to half its maximum value. Since for typical parameters $N \approx 50$, and $R_c \approx 1\ \mu$m comparable to the optical resolution, the spatially resolved probe absorption provides an excellent signature for the presence of a single Rydberg atom within a dense gas.

To apply this scheme to real experiments one also has to analyze the influence of noise. We identify two major sources: one can be attributed to photon-shot noise while a second contribution is associated with intrinsic atomic density fluctuations [20]. Both noise sources can

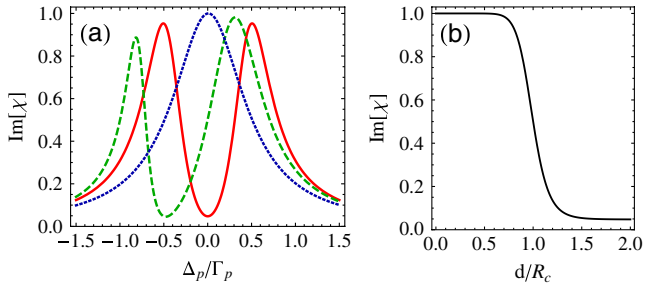

FIG. 2 (color online). Imaginary part of the susceptibility. (a) $\text{Im}[\chi]$ as a function of probe detuning for $\Omega_c = 1$, $\Gamma_c = 0.05$, and $\Delta_c = 0$ (in units of Γ_p) for various distances from the Rydberg atom. The solid line is for $d \to \infty$, the dashed line corresponds to $d = R_c$, and the dotted line is for $d = R_c/2$. (b) $\text{Im}[\chi]$ as a function of distance from the Rydberg atom with $\Delta_p = 0$.

be accurately described as Poissonian processes. This suggests that the signal-to-noise ratio can be made arbitrarily large for large intensity and large density. However, to neglect interactions between background atoms we require the probability to find more than one atom in the $|r\rangle$ state within the range of background-background interactions R_c' to be $\lesssim 1$ (for the states we consider $R_c' \approx R_c$). This constraint imposes a relationship between the maximum density of background atoms and the maximum probe intensity $n_{2D} \lesssim \Omega_c^2/\pi R_c'^2 \Omega_p^2$. Above this critical density the contrast of the image would decrease due to the blockade effect, where only one atom can contribute to the EIT signal, while the remainder couple resonantly to the probe laser [11,21]. In general, the maximum signal-to-noise ratios are achieved for large coupling strengths Ω_c and long exposure times τ, but in practice these will be limited by the available laser power and by the required time resolution, which should be compared to the typical lifetime of a Rydberg atom (~ 100 μs).

To show the potential of this imaging scheme we have carried out numerical calculations of the EIT imaging process on simulated distributions of Rydberg atoms excited from a quasi-2D ideal gas. This situation can be realized with an optical dipole trap made using cylindrically focused Gaussian beams. Of particular interest for current experiments is the possibility to observe strong spatial correlations between Rydberg atoms induced by interactions in an otherwise disordered gas [14,18,22].

We use a simple semiclassical model to simulate the excitation of Rydberg atoms during a chirped pulse [20]. The model is closely related to those used to describe optical control of cold collisions [23,24]. We consider a thermally distributed gas of 25 000 ^{87}Rb atoms with a peak density $n_{2D} = 40$ atoms/μm^2 and a cloud radius of $\sigma = 10$ μm. Each atom can be in either the electronic ground state or a Rydberg state. We assume isotropic van der Waals interactions between Rydberg atoms with a $C_6 = 2\pi \times 50$ GHz μm^6, typical for the $55S$ state [25]. The detuning of the excitation laser is swept from 0 to $+200$ MHz within 6 μs with an effective Rabi frequency of $\Omega = 2\pi \times 2.0$ MHz. During each time step atoms can undergo a transition to the Rydberg state with a probability estimated from the Landau-Zener formula [26]. Successive excitation events are treated independently; however, previously excited atoms influence successive transitions through the Rydberg-Rydberg interactions. This model also includes the effects of mechanical forces between Rydberg atoms by simultaneously solving the classical equations of motion for each Rydberg excited atom.

We then calculate absorption images of the simulated Rydberg distributions by numerically solving the optical Bloch equations for the probe atoms at each spatial position, accounting for the level shifts produced by all Rydberg atoms. We assume the atoms are nearly stationary during the imaging process, which requires temperatures below ≈ 10 μK. From the mean intensity at each pixel we generate Poisson distributed photon-shot noise. Similarly, a reference image is generated with uncorrelated noise for background division. Figure 3 shows calculated single-shot absorption images without and with the coupling laser. Each pixel corresponds to a region of $(0.5\ \mu\text{m})^2$ in the plane of the atoms and we assume a numerical aperture of 0.25 and an exposure time of 10 μs. For the probe atoms, we take the ^{87}Rb states, $|5S_{1/2}, F = 2, m_F = 2\rangle$ for the ground state, $|5P_{3/2}, F = 3, m_F = 3\rangle$ for the intermediate state, and $|r = 28S\rangle$ for the excited state. The decay rates are $\Gamma_p = 2\pi \times 6.1$ MHz and $\Gamma_c \approx 2\pi \times 10$ kHz, and for the coupling laser we assume $\Omega_c = 2\pi \times 50$ MHz. Laser linewidths of $2\pi \times 1$ MHz were assumed for both probe and coupling lasers. The interaction coefficient between $|55S\rangle$ and $|28S\rangle$ states was calculated as $C_6(28S - 55S) = -2\pi \times 8.7$ MHz μm^6 giving $R_c = 0.59$ μm. Interactions between background atoms are taken as $C_6(28S - 28S) = 2\pi \times 10.1$ MHz μm^6 ($R_c' = 0.61$ μm). For these parameters the optimal signal-to-noise ratio is obtained for $n_{2D} \approx 40$ atoms/μm^2. The probe Rabi frequency ($\Omega_p = 2\pi \times 5.8$ MHz) is chosen such that on average the $|r\rangle$ state density remains below 1 per $\pi R_c'^2$. Such parameters are readily achieved in current experiments with quasi-2D atomic gases [27].

In the background region of the image the signal is dominated by photon-shot noise, while at the center atom-shot noise dominates. With the coupling laser on the probe atoms are rendered mostly transparent, except for regions of high absorption around each Rydberg atom [Fig. 3(b)]. The locations of the individual Rydberg atoms are clearly resolved in the image as bright (absorbing) spots with a spatial extent of 2.3 μm FWHM comparable to the assumed optical resolution. One can easily envisage higher resolutions using state-of-the-art imaging systems [7], with the fundamental limit given by the density of

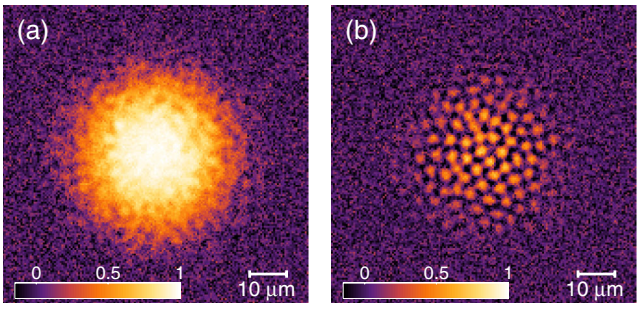

FIG. 3 (color online). Simulated absorption images of atom distributions including photon-shot noise and atomic density fluctuations. In (a), without the coupling beam, a regular absorption image of the probe atoms is obtained. The color code indicates absorption. With the coupling on (b) the probe atoms are rendered transparent, except for those in the vicinity of a Rydberg atom. Parameters of the simulation can be found in the text.

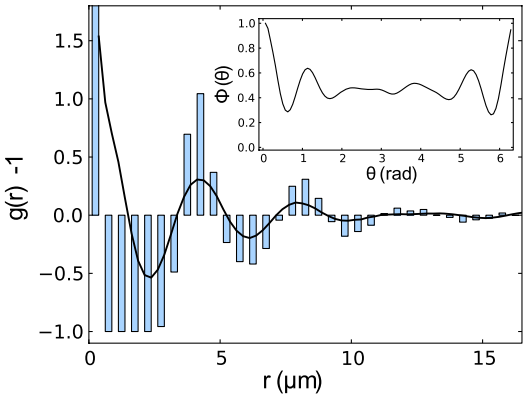

FIG. 4 (color online). Pair distribution and angular correlation function of 15 simulated Rydberg images. The solid black line shows $g(r) - 1$ computed from the absorption images for 15 realizations. The shaded bars show $g(r) - 1$ taken directly from the simulated Rydberg atom coordinates with a bin size of 0.5 μm. The clear shell structure which reflects translational order between nearest and next-nearest neighbors is preserved by the images. The inset shows the angular correlation function for the radius of the first shell.

background atoms surrounding the impurities. The signal-to-noise ratio of our images is sufficiently high that we can fit the position of each Rydberg atom with subpixel precision.

From the simulated images, we see that the distribution of Rydberg atoms appears highly correlated, reproducing some of the features of a full quantum mechanical treatment [18]. To characterize the translational order of the simulated Rydberg distributions, we calculate the pair distribution function $g(r)$ [20] from 15 simulated images (Fig. 4). To account for the inhomogeneous density distribution we also normalize by the autocorrelation of the mean image. For a random distribution of atoms $g(r) \approx 1$. Larger correlation values indicate an enhanced probability to find two Rydberg atoms at a given separation, while lower values indicate the absence of pairs. Since there is no preferred orientation in our system $g(r)$ takes on cylindrical symmetry. We clearly observe a shell with $g(r) \approx 0$ at a radius of $\sim$2.5 μm which reflects the strong blockade of excitation due to Rydberg-Rydberg interactions. At larger distances, we observe two positive-correlated shells (around 4 and 8 μm), which indicate translational correlations between nearest and next-nearest neighbors. The observed shell structure decays rapidly indicating the absence of true long-range order. We note very similar behavior of $g(r)$ for the raw atom positions (shaded bars). From this we conclude that the information regarding density-density correlations can be reliably extracted from the images, even under realistic imaging conditions.

We have also computed the angular correlation function $\Phi(\theta)$ at the radius of 4 μm (inset Fig. 4). This gives the probability, starting from an atom to find two neighbors forming an angle θ. We observe the presence of two peaks at $\sim\pi/3$ and $\sim 5\pi/3$ rad, reflecting the sixfold symmetry present among most nearest neighbors. Even more information could be obtained from these images by studying higher-order correlation functions, or by first estimating the Rydberg atom positions to fully characterize the many-body state.

Our new imaging method provides the means to optically image individual particles within a dense atomic gas using Rydberg state electromagnetically induced transparency. The EIT imaging scheme allows for single-shot, nondestructive, and time resolved images of many-body states. The conditions we find to optimize the signal closely match those of current cold atom experiments. To illustrate the potential of this new imaging scheme, we have carried out numerical simulations of Rydberg atoms excited from a quasi-2D gas and calculated the corresponding absorption images. We can foresee numerous other applications of the EIT imaging method. For example, Rydberg state EIT has already been used to measure spatially inhomogeneous electric fields near a surface [12]. Another exciting prospect would be to directly image single ions within an atomic gas [28]. The presence of a single ion at a distance of 1 μm would cause a shift of the $|21S\rangle$ states of a ^{87}Rb atom cloud of 12 MHz, which could be readily observed using EIT imaging. Closely related ideas could be used to realize a single-atom optical transistor [29] or to impose nonclassical spatial correlations onto the light field [30].

We thank J. Evers, B. Olmos, and I. Lesanovsky for valuable discussions. This work is supported in part by the Heidelberg Center for Quantum Dynamics and the Deutsche Forschungsgemeinschaft under WE2661/10.1. S. W. acknowledges support from the EU Marie-Curie program (Grant No. PERG08-GA-2010-277017). M. R. D. S. V. acknowledges support from the Alexander von Humboldt Foundation.

Note added.—Recently, we became aware of related work [17].

*whitlock@physi.uni-heidelberg.de
†weidemueller@uni-heidelberg.de

[1] D. Meschede and A. Rauschenbeutel, Adv. At. Mol. Opt. Phys. **53**, 75 (2006).
[2] W. E. Moerner, Proc. Natl. Acad. Sci. U.S.A. **104**, 12 596 (2007).
[3] D. Leibfried, R. Blatt, C. Monroe, and D. Wineland, Rev. Mod. Phys. **75**, 281 (2003).
[4] E. Betzig and R. J. Chichester, Science **262**, 1422 (1993); X. S. Xie and R. C. Dunn, Science **265**, 361 (1994).
[5] A. Yazdani *et al.*, Science **275**, 1767 (1997); S. H. Pan *et al.*, Nature (London) **403**, 746 (2000).
[6] D. Schrader *et al.*, Phys. Rev. Lett. **93**, 150501 (2004); K. D. Nelson, X. Li, and D. S. Weiss, Nature Phys. **3**, 556

(2007); H. Häffner *et al.*, Nature (London) **438**, 643 (2005).
[7] T. Gericke *et al.*, Nature Phys. **4**, 949 (2008); W. S. Bakr *et al.*, Nature (London) **462**, 74 (2009); C. Weitenberg *et al.*, Nature (London) **471**, 319 (2011).
[8] W. Nagourney, J. Sandberg, and H. Dehmelt, Phys. Rev. Lett. **56**, 2797 (1986).
[9] J. Bochmann *et al.*, Phys. Rev. Lett. **104**, 203601 (2010); R. Gehr *et al.*, Phys. Rev. Lett. **104**, 203602 (2010); N. Brahms *et al.*, Nature Phys. **7**, 604 (2011).
[10] M. Gierling *et al.*, Nature Nanotech. **6**, 446 (2011).
[11] A. K. Mohapatra, T. R. Jackson, and C. S. Adams, Phys. Rev. Lett. **98**, 113003 (2007); K. J. Weatherill *et al.*, J. Phys. B **41**, 201002 (2008); J. D. Pritchard *et al.*, Phys. Rev. Lett. **105**, 193603 (2010); H. Schempp *et al.*, Phys. Rev. Lett. **104**, 173602 (2010).
[12] A. Tauschinsky *et al.*, Phys. Rev. A **81**, 063411 (2010).
[13] R. Löw *et al.*, Phys. Rev. A **80**, 033422 (2009).
[14] T. Cubel Liebisch, A. Reinhard, P. R. Berman, and G. Raithel, Phys. Rev. Lett. **95**, 253002 (2005); T. Amthor, C. Giese, C. S. Hofmann, and M. Weidemüller, Phys. Rev. Lett. **104**, 013001 (2010); M. Viteau *et al.*, Phys. Rev. Lett. **107**, 060402 (2011).
[15] A. Schwarzkopf, R. E. Sapiro, and G. Raithel, Phys. Rev. Lett. **107**, 103001 (2011).
[16] M. Müller *et al.*, Phys. Rev. Lett. **102**, 170502 (2009).
[17] B. Olmos, W. Li, S. Hofferberth, and I. Lesanovsky, Phys. Rev. A **84**, 041607 (2011).
[18] H. Weimer, R. Löw, T. Pfau, and H. P. Büchler, Phys. Rev. Lett. **101**, 250601 (2008); T. Pohl, E. Demler, and M. D. Lukin, Phys. Rev. Lett. **104**, 043002 (2010); J. Schachenmayer, I. Lesanovsky, A. Micheli, and A. J. Daley, New J. Phys. **12**, 103044 (2010); R. M. W. van Bijnen *et al.*, J. Phys. B **44**, 184008 (2011).
[19] M. Fleischhauer, A. Imamoglu, and J. P. Marangos, Rev. Mod. Phys. **77**, 633 (2005).
[20] See Supplemental Material at http://link.aps.org/supplemental/10.1103/PhysRevLett.108.013002 for more information on the influence on noise, the Rydberg excitation model, and the correlation analysis.
[21] C. Ates, S. Sevinçli, and T. Pohl, Phys. Rev. A **83**, 041802 (R) (2011).
[22] F. Robicheaux and J. V. Hernández, Phys. Rev. A **72**, 063403 (2005).
[23] K.-A. Suominen, J. Phys. B **29**, 5981 (1996).
[24] M. L. Wall, F. Robicheaux, and R. R. Jones, J. Phys. B **40**, 3693 (2007).
[25] K. Singer, J. Stanojevic, M. Weidemüller, and R. Côté, J. Phys. B **38**, S295 (2005).
[26] C. Wittig, J. Phys. Chem. B **109**, 8428 (2005).
[27] A. Görlitz *et al.*, Phys. Rev. Lett. **87**, 130402 (2001).
[28] A. T. Grier, M. Cetina, F. Oručević, and V. Vuletić, Phys. Rev. Lett. **102**, 223201 (2009); C. Zipkes, S. Palzer, C. Sias, and M. Köhl, Nature (London) **464**, 388 (2010); S. Schmid, A. Härter, and J. H. Denschlag, Phys. Rev. Lett. **105**, 133202 (2010).
[29] J. Hwang *et al.*, Nature (London) **460**, 76 (2009).
[30] S. Sevinçli, N. Henkel, C. Ates, and T. Pohl, Phys. Rev. Lett. **107**, 153001 (2011).